The position of the `one-eighth' anomaly within the high-temperature superconductivity problem: matters concerning stripes and domains, Jahn-Teller effect and negative- ***U*** behaviour

1998 J. Phys.: Condens. Matter 10 3387

(http://iopscience.iop.org/0953-8984/10/15/015)

J. Phys.: Condens. Matter **10** (1998) 3387–3410. Printed in the UK PII: S0953-8984(98)88922-4

The position of the 'one-eighth' anomaly within the high-temperature superconductivity problem: matters concerning stripes and domains, Jahn–Teller effect and negative-U behaviour

John A Wilson

H H Wills Physics Laboratory, University of Bristol, Tyndall Avenue, Bristol BS8 1TL, UK

Received 31 October 1997

Abstract. The subject of mixed-valence charge segregation in HTSC materials is further examined. The self-organized microstructural details are explored including 1D/2D crossover. Neutron and extended x-ray absorption fine-structure results provide the basis for this analysis. The Jahn–Teller effect is seen as a crucial element in the 'charge/spin'-separation structuring. On cooling, the emergent resonating-valence-bond-type magnetic organization of the divalent subsystem assists greatly in preparing (if not pre-pairing) the overall system for high-temperature superconductivity. Under the action of the negative-U centres of the high-valence subsystem established in the domain boundaries, the system can evolve naturally with doping and cooling from $d_{x^2-y^2}$ towards greater s-wave-type content of the HTSC order parameter.

1. Introduction

This paper addresses the well-known 'one-eighth problem' and matters surrounding it in more detail than was possible in [1a] and the subsequent addendum. Since that article appeared, considerably more data have become available and the questions raised by 'stripe phase' formation have become better formulated and more widely considered. In fact the whole question of mixed-valence inhomogeneity and microstructure is one which must be brought to centre stage if a proper resolution is to be made of the HTSC phenomenon. As discussed at length in [1a], that includes a recognition of the true form of the superconducting order parameter, and likewise of the real nature of the anomalous normal-state transport behaviour. To this end, attention has been confined here in the first instance to the long-researched one-eighth anomaly. In complex systems it is absolutely essential that the full intricacies of the structural condition be acknowledged from the start. The acquisition of charge-segregated domain structures is readdressed, making explicit the role that the Jahn–Teller effect and ordered magnetic states play in the development of such forms in the mixed-valence cuprates. Section 2 introduces these sub-topics in some detail and tries to consolidate the crystallographic basis from which they can be discussed. In section 3.1 we introduce the question of 1D versus 2D domains and address what is at stake in the crossover encountered at around $x = 1/8$ in the relationship between doping content and domain size (i.e. the supercell wavevector). In section 3.2 we look at the details emerging from local structural probes, particularly EXAFS, which tightly control the formulation of supercell models. These supercells clearly are strongly perturbed by static disorder and dynamic

0953-8984/98/153387+24$19.50

fluctuation. In section 4 we examine which fluctuations are essential to the promotion of T_c and which impair it. The appearance of RVB-type behaviour within the domains is seen as crucial in securing spin gapping (and hence minimizing pair breaking), whilst at the same time it prepares spin pairs for incorporation into the coherent superfluid. The latter, we maintain, is instigated and sustained by negative-U coupling within the high-valence, spin-free, domain boundaries [1]. Finally, section 5 deals with the role played by density-of-states peaks in promoting HTSC. It emphasizes that the important features indeed present near E_F in HTSC materials are to be recognized as being primarily many body in character, and not simple DOS peaks. The nature of these mixed-valence metals is so perturbed by the inhomogeneous microstructure that such standard features cannot play a determinative role, and the evident uniformity of behaviour across the whole family of HTSC materials well expresses this.

2. Background to the 'stripe phase' formation and to the 'one-eighth' problem

From the outset of HTSC it has been emphasized in [1a–1g] that stoichiometry-induced mixed valence in the cuprates, as in other 3d oxides, establishes a significantly inhomogeneous two-subsystem environment for the principal cation. The degree of inhomogeneity naturally is somewhat less in delocalized systems like $(La/Sr)_2CuO_4$ and $HgBa_2CuO_{4+\delta}$ than in say $(La/Sr)_2NiO_4$ and $(La/Ca)MnO_3$. Nevertheless, since single-valent ($3d^9$) La_2CuO_4 and ($3d^8$) $LaCuO_3$ are still quite hard Mott insulators (no delocalization to 10 GPa), the Madelung differentiation of site environments in the mixed-valence HTSC cuprates remains very significant. This has been directly registered using many different kinds of local probe (e.g. NQR [2], EXAFS [3], PDF [4]). In reference [1f] it was pointed out that for the given layered structures of the HTSC systems, when one takes one charge substituent to affect four nearest-neighbour Cu coordination units in the crucial CuO_2 chessboard array, the optimal T_c-value within a given system, arising always at '$x = 0.16$', becomes associated with the point at which (for random doping) percolation pathways through the mixed-valence array first become established over the subsystem being so driven towards trivalence. Formed simultaneously at this level of substitution is the maximal interface between the two subsystems created; this further facilitates dynamic inter-subsystem particle transfer and metallic, unactivated charge transport (see figure 4 in reference [1f]).

To a first approximation the time-averaged site-charge counts differentiate into just two types, closely characterized in regard both to local bonding and to on-site magnetic moment. Currently involved for the d^8/d^9 cuprates are the two e_g-symmetry-derived antibonding $pd\sigma^*$ wavefunctions—termed loosely d_{z^2} and $d_{x^2-y^2}$. For 'd^8' Cu_{III} (as with Au_{III}) the couple of σ^*-electrons in question become accommodated into the low-spin condition $(p_z d_{z^2}\sigma^*)^2$—this in contrast to the high-spin, Hund's rule condition exhibited by d^8 Ni_{II} in the more ionic situation of La_2NiO_4 or NiO. Within the cuprate layered structures the former condition arises in part from the small average Cu–O basal bond length imposed upon the overall system by the 'majority' d^9 Cu_{II} sites; this small value is itself a consequence of the on-site Jahn–Teller (J–T) effect. In the J–T process the octahedral coordination-unit geometry becomes strongly broken so as to eliminate the degeneracy between the above two e_g states. Always the local J–T effect that is associated with e_g-symmetry σ/σ^*-bonding/antibonding states (i.e. at high spin, d^4; low spin, d^7; d^9 for octahedral or square-pyramidal coordination) is much more marked than is the case with π-type-interacting, 'non-bonding' t_{2g} states (namely at d^1; low spin, d^5; high spin, d^7). The much-enhanced antibonding character of the $d_{x^2-y^2}$ (e_g) state, coming from the very strong basal bonding/antibonding $p_{x,y}d_{x^2-y^2}\sigma/\sigma^*$

interaction, taken in conjunction with the accompanying strong relaxation of the d_{z^2}-governed apical Cu–O bond length, forms a key aspect of the HTSC materials. What results is that the d_{z^2}-based antibonding states always are fully occupied, falling entirely below their otherwise degenerate $d_{x^2-y^2}\sigma^*$ partners. All present discussion of HTSC focuses upon the latter states, somewhat less than half-full on average over the two subsystems.

The on-site Jahn–Teller effect tends to disappear in more delocalized metals, such as CuS_2, but very significantly in the HTSC cuprates the J–T effect is greatest in just those systems wherein T_c^{max} is highest [5]. For example in $HgBa_2CuO_{4+\delta}$ (at the δ yielding T_c^{max}) the basal contraction to Cu–O = 1.94 Å becomes partnered by an apical elongation to 2.78 Å. In the cuprates the very marked antibonding form of the upper e_g state issues from the high degree of degeneracy between the interacting parent oxygen p and copper d states, just prior to completion there for copper of the 3d shell. With cuprate band structures there ensues a very considerable width to the $pd\sigma^*$ band of $d_{x^2-y^2}$ symmetry. In simple LDA calculations [6] that width (though clearly overstated in these at ~4 eV) establishes the marked difference in delocalization and magnetism between the cuprates and their nickelate or cobaltate analogues (see [7]).

The incurred level of upward ejection of the $d_{x^2-y^2}\sigma^*$ state in the HTSC cuprates, and its subsequent strong reversion towards the semicore during fluctuational attainment of the filled-shell configuration $d^{10}(p^6)$—particularly as encountered in the higher-valence subsystem—we have made the basis of an electronic negative-U modelling of the HTSC phenomenon, presented at length in our earlier papers [1]. It is not the intention in the first place directly to pursue that matter. Rather we wish simply at this point to emphasize the importance of the Jahn–Teller effect in regard to the complementary matter of valence segregation and of 'stripe phase' organization within the layered mixed-valence cuprate 'metals' *above* T_c.

Some time ago we reported [8] the direct observation by electron microscopy of a bulk spinodal decomposition of $La_2CuO_{4.03}$ (LCO+) into a roughly 50:50 sequential mixture of regions of near-stoichiometric La_2CuO_4 and compensating $La_2CuO_{4.06}$—with a typical length scale 300 Å. That study was undertaken because we were intrigued to understand how this starting material was able so closely to mimic the superconducting properties of optimally doped $(La/Sr)_2CuO_4$ (refer to [9] for a review of the current situation). Bulk segregation proceeds in LCO+ by migration of the metallizing excess oxygen, and this occurs at the remarkably low temperatures of between 300 and 200 K. Easy ionic migration at such temperatures has to be assisted by energies other than that of simple thermal activation. The extra energies active in the system are the relevant Jahn–Teller electronic and strain energies as well as the magnetic energy. LCO+ like LSCO is moment compensated when/where optimally doped, though of course stoichiometric La_2CuO_4 and likewise this component in spinodally decomposed $La_2CuO_{4.03}$ show relatively free local moment behaviour well above room temperature, followed by standard 2D and 3D antiferromagnetic coupling at lower temperatures.

Matching the work of Tranquada *et al* on the nickelates and on $(La/Nd/Sr)_2CuO_4$ [10], we in addition have since examined too [1a] the closely related matter of organized 'stripe phase' formation in the HTSC cuprates (as distinguished from the above 'bulk' phase separation). It was demonstrated in appendix B to reference [1a] that the incommensurate spin scattering detected in the inelastic neutron scattering work on LSCO by Mason, Aeppli, Hayden and co-workers [11], and discussed by them in terms of incipient SDW formation under Fermi surface nesting [12], is much better seen as an attempt at valence segregation, this affecting both charge and spin organization. The segregation materializes here in the form of electron-depleted spin-free bands separating intervening spin-coupled plaquettes

of nominally divalent material. For the given stoichiometries the suggested two-sublattice ordering patterns are demonstrated in [1a] to be compatible with the incommensurate q-vectors observed by neutron scattering, as well as other magnetic characteristics displayed. The situation will be expanded upon below. Such an interpretation would appear to be one much more in keeping with the given degree and nature of the nesting present within the LSCO band structure than is a standard SDW interpretation. The skewing of the instability wavevector away from $\boldsymbol{Q} = (0.5, 0.5)\pi$, when taken to proceed from charge and spin ordering under *local* Jahn–Teller-driven strain and magnetic terms, represents a more robust route to the observed effects. Standard nesting is most effective where band dispersion is *greatest* on the Fermi surface [13]—potentially here along $(k, k, 0)$—whilst in the cuprates the nesting would appear principally to be of the saddle-point variety relating to $\{\pi/2, 0, 0\}$. At the saddles the DOS is raised appreciably. Moreover $\chi(q)$ is also large there because $\chi^0(q)$ is then in register with the antiferromagnetic superexchange of the Cu–O–Cu 180° linkages (see figure 1 in reference [1d]).

A domain condition, when fully regularized, already by $x = 0.125$ (i.e. by the substantial hole content of 1/8) comes to generate a very compact array as portrayed in figure 1 (taken from reference [1a]). Here two unit cells of non-magnetic wall (8 Å) are followed by three two-cell plaquettes of coupled spins, to yield an overall $8a^T$ repeat of 31 Å. This, as will be discussed, is a very comparable spatial apportionment to that published initially for Bi-2212 and subsequently LBCO by Bianconi and co-workers arguing from their EXAFS data [14]—though not by them assigned the same detailed charge arrangement as in our own work (see section 3 below). Bianconi and co-workers anticipate such a *regular* striped organization to be of crucial import to the HTSC process itself, but from our perspective that would seem to constitute an unnecessary constraint. Nonetheless it is of great interest to examine how the incipient mixed-valence micro-order can influence the superconducting state; recall that its characteristic length scale is virtually identical to the 0 K superconducting coherence length. The restricted size of the latter is of course what confers upon the HTSC cuprates the high values of H_{c2}, $\Delta(0)$ and T_c, and is the direct signature of a local pairing mechanism.

The influence of the details of the lattice upon cuprate superconductivity has been raised many times [15], especially the issue of lattice instability, since this in conventional superconductors is perceived to open a way to higher electron–phonon coupling, and thereby to higher T_c-values. Because HTSC first emerged with the LBCO system, and because the latter exhibits clear structural instability, most investigations have centred upon this system. Particular attention [16] has been paid to the Ba $x = 1/8$ composition, in the vicinity of which one encounters upon cooling the following structural sequence:

$$\begin{array}{ccccc} \text{HTT } (I4/mmm) & \longrightarrow & \text{LTO}_1\ (Abma) & \longrightarrow & \text{LTT } (P4_2/ncm) \\ \text{D}_{4\text{h}}^{17}\ \{Z=1\} & & \text{D}_{2\text{h}}^{18}\ \{Z=2\} & & \text{D}_{4\text{h}}^{16}\ \{Z=2\times 2\} \end{array}$$

(with additionally LTO_2 $(Pcnn)$ $\text{D}_{2\text{h}}^{10}$ as an intermediary between the latter two if >15% of the La^{3+} is replaced by the smaller Nd^{3+}). For LSCO a transition from HTT to LTO_1 occurs that is similar to the one in LBCO, although weaker and at lower temperature, and the same is the case for the second transition seen when Nd is present.

It is well known that in LBCO, in close proximity to the 0.125 composition, there in fact occurs a remarkable sharp *suppression* of the superconducting response, very evident both in $\sigma(x, T)$ and $\chi(x, T)$ [17]. At other neighbouring stoichiometries all of the above structure types have been demonstrated to support superconductivity [18]. Indeed it has been shown theoretically that the relatively small band-structural DOS changes introduced with the various above breaks in crystal symmetry cannot in the main be held responsible for the collapse in superconducting behaviour witnessed in LBCO close to $x = 0.125$ [19,

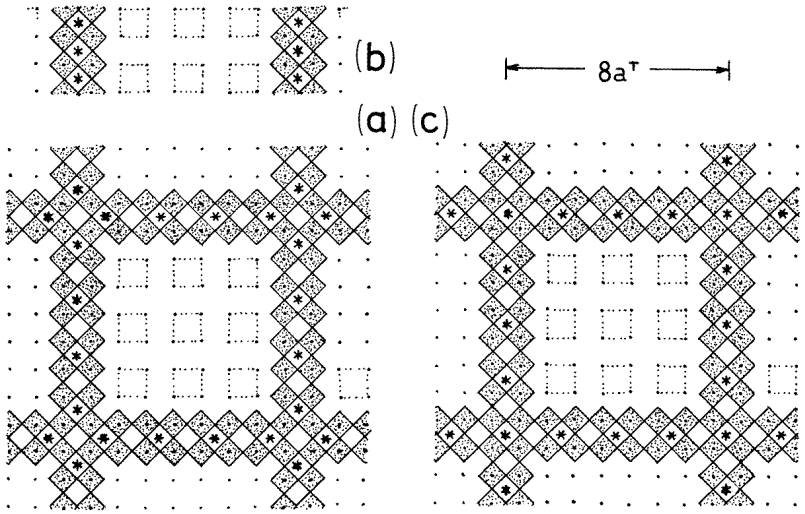

Figure 1. Regularized 'stripe phase'-type structures appropriate to $(La_{2-x}Ba_x)CuO_4$, $x = 0.125$: (a) the 2D modelling of [1a], based primarily on neutron scattering results; (b) the 1D modelling of [14b], based primarily on EXAFS data. In these valence-segregated models the two different subsystems are indicated through the shading of the basal CuO_2 squares of the higher-valence one within this electronically inhomogeneous mixed-valence system. In model (a), note that each dopant charge (centred on $*$) has been distributed over four contiguous Cu coordination units, whilst in model (b) the charge is more concentratedly distributed, each unit charge being associated now with just two Cu coordination units. In the 1D model the dopant concentration is immediately seen to be reciprocally equal to the spacing of the stripes, and hence numerically equal to the wavevector of the stripe periodicity. In the 2D case of part (b) the same numerology holds; i.e. (charge/cell)/(Cu atoms/cell)—that is, here, $8/8^2$—$=1/8$, = charge/Cu atom.

Although the charge concentration and cell wavevector both here equal 0.125, note that this simple equivalence is broken in the case of part (c). There the charges of part (b) have been slipped so as to centre the corners of the 2D supercell. For that setting the wavevector remains 0.125, but the charge concentration now falls to $7/8^2$ or 0.1093.

The above structures are not discommensurate in the sense that there is no phase slippage here across the domain boundaries *if* simple 'up/down' spin sequencing is presumed for the local magnetic ordering within the unshaded low-valence subsystem—contrast figure 8, later. Between the boundaries the spins are shown coupled into four-spin plaquettes. The true circumstance is not so statically or so simply regularized. The Ba cations at low temperature are not easily transposed from their otherwise random distribution (see figure 4 in the first of the references [1f] for the case of $x = 1/6$). By contrast, in $La_2CuO_{4+\delta}$ (and probably in similarly super-oxygenated HTSC systems) the excess oxygen ions can migrate down to 200 K, through a highly defective sublattice. (NB In this and all subsequent figures the Cu–O bonds are aligned horizontally and vertically.)

20]. Not only can the standard electron–phonon coupling not be so sharply altered, but one should moreover recall that by $x = 1/6$ (i.e. at T_c^{max}) the oxygen isotope effect exponent α is observed to drop almost to zero [21], clearly intimating an electronic mechanism then to be dominant.

A crucial point to register is that the above *lattice* instabilities in the HTSC cuprates are fundamentally unrelated to questions of Fermi nesting since they occur even more strongly in the corresponding nickelates, cobaltates etc, and these are Mott insulating. Structural analysis would indicate that the instabilities arise in response to packing mismatch between the chessboard and rock-salt segments of the A_2BO_4 layered structure centred upon the

two different cations. The strain can be relieved by the various coherent coordination-unit tiltings within the TM–O basal network of corner-linked octahedra. The observed patterns of tilting have satisfactorily been modelled in soft-mode, mean-field fashion using standard Ginzburg–Landau theory [16]. In the cuprate case the elongation of the apical bond is observed in fact to alter very little from one structure to the next [22], signalling thereby that the final electron is not much involved. Accordingly the strange electronic condition in LBCO centred closely upon $x = 0.125$ has to emerge from more distinctive physics, associated specifically with the mixed-valence inhomogeneity and associated metallicity.

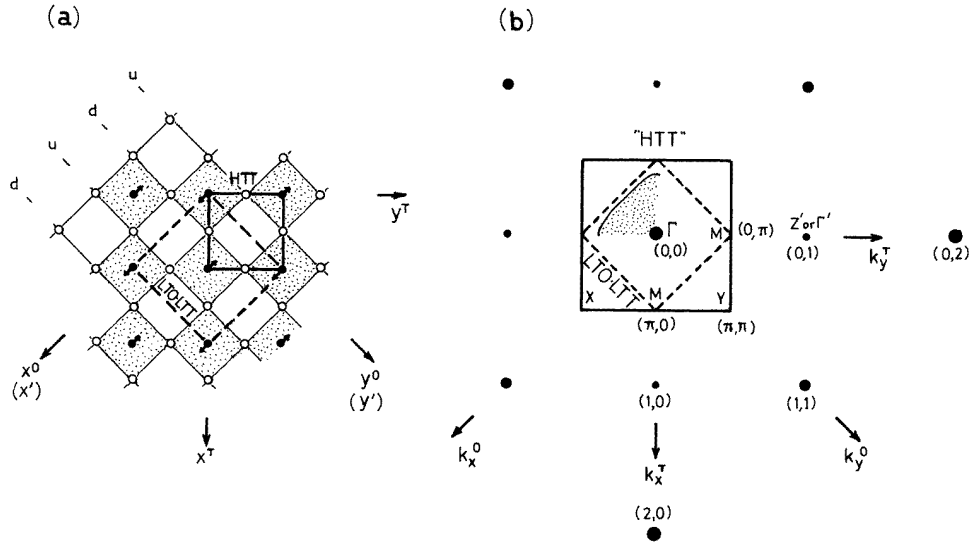

Figure 2. Portrayals in (a) direct and (b) reciprocal space of the inter-relationship between the various structures displayed by LBCO, suppressing all c-axis details and any slight orthorhombic distortion of the basal plane. See the main text for space group details. We are adhering, note, to the *Abma* choice for the low-temperature orthorhombic phase LTO_1 detailed earlier in [8], wherein $a^O > b^O$ and b^O defines the tilt axis. Note also in regard to the vertical sections given in figure 1 of the first of references [1f] of the LBCO LTO structure that a^O runs horizontally in part (c) and b^O runs horizontally in part (d). The LTO tilts of the copper coordination-unit octahedra have been indicated in part (a) by small tabs. The (average) tilts in LBCO fall from 5 to 0° with substitution x [22].

Shown in (b) is an indication of the underlying 2D Brillouin zones, plus the 2D LBCO Fermi surface in the HTT phase with its saddles at $\{\pi, 0\}$. Note that in the true, 3D, body-centred tetragonal HTT phase, $\{1, 0\}$ reciprocal-lattice points are actually Z′ points and are diffraction forbidden in HTT. By the LTT phase, besides the strong $\{1, 1\}$ family and weaker $\{1, 0\}$ family of spots becoming allowed, further much weaker diffraction spots additionally appear at the points $\{\pi, \pi\}$ important to antiferromagnetic discussions (see figure 4, later). Misleadingly the latter k-points in the B.Z. often are labelled X, Y, being so designated with regard to the 45°-rotated $k_{x',y'}$-axes of pure La_2CuO_4 in its R.T. b.c.t. HTT phase: these axes run from the central Γ point (0, 0) to the nearest true Γ points $\{1, 1\}$. This confusing terminology recurs in regard to BSCCO-2201 etc. (For fuller details of the packing of such b.c.t. B.Z.s, refer to figures 5 and 7 in our paper [61].) Note that $Hg_xBa_2CuO_{4+\delta}$ is simple tetragonal and is a potential HTSC archetype provided that the Hg content can more readily be brought to unity.

Back in 1989, rather hesitantly it was suggested in [1e] that what is occurring at $x = 1/8$ might be the consequence of a Wigner-related crystallization of the Fermi sea, the doped holes still being quite heavy there and polaronic in character. Such a charge ordering might

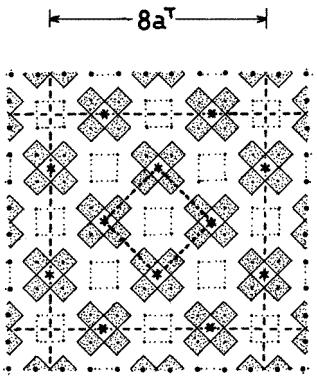

Figure 3. Regular crystallization of carriers for $x = 0.125$, represented in manner of figure 1(a). The central 45°-rotated unit cell is of edge $2\sqrt{2}a^T$, or twice that for the LTO/LTT structure. To convert from this Wigner array to the domain condition of figure 1(a) the 'out-of-position' central charges have only to migrate ~8 Å—but of course then be systematically constrained.

substantially gap the Fermi surface at $x = 1/8$, the repeat cell involved being in step with the crystalline LTT periodicity (figure 2). Indeed it is known that the resistivity rises—see [17a]. However, more recently it has been demonstrated that the events are to be associated as much with developments in the magnetic order as with charge ordering. Up to a point we now are in a position to see how this comes about. Figure 3 portrays the very limited level of charge motion needed to pass from a simple Wigner array to the corresponding domain array for a doping of $x = 1/8$ (figure 1(a))—though, of course, in systematic fashion. Demanding close attention as well below will be the corresponding (though significantly weaker) events which develop in LSCO and apparently there centred upon the at first sight incommensurate x-value of 0.115 [23].

One of the nicest experiments to demonstrate the predominantly electronic character of what is happening in the above is that of Maeno *et al* [24] in which they partially counter-substitute for the Ba^{2+} of LBCO with Th^{4+}. It is observed that, despite the increase in net dopant content, the magnetic and superconducting anomalies remain closely anchored to the hole content of 1/8. A similar result more recently has been secured by employing LBCO samples loaded under pressure to various excess oxygen stoichiometries [25].

It is directly apparent in the domain phase condition adopted that the local antiferromagnetic order which has been deduced from μSR [26] as developing at $x = 0.125$ in between the (higher-valence) domain walls of segregated holes acts to impair superconductivity and ordinary conductivity alike. It is found possible for this magnetism of the Cu_{II} subsystem to be more intensively promoted through a partial replacement of the La^{3+} with $Nd^{3+}(f^3)$, and then beyond a 15% Nd substitution level even the strontium compound never becomes superconducting across a wide range of Sr doping from $x = 0.10$ to 0.15 [27]. By using μSR for these Nd-substituted systems it once again becomes possible directly to make manifest that two subsystems are present in the materials [27]. Indeed as was noted at the outset it long has been evident from many local probes, such as NQR [2], EXAFS [3] and PDF correlations [4], that two readily differentiated types of Cu site exist in LBCO and LSCO at all compositions—at least up to $x(T_c^{max})$ [2]. Only, however, with k-space diffraction data can one obtain a full view of the longer-range structural and magnetic organization arising [28]. With regard to the form of the *spin* array the extensive neutron scattering results from LSCO [11] yield invaluable information.

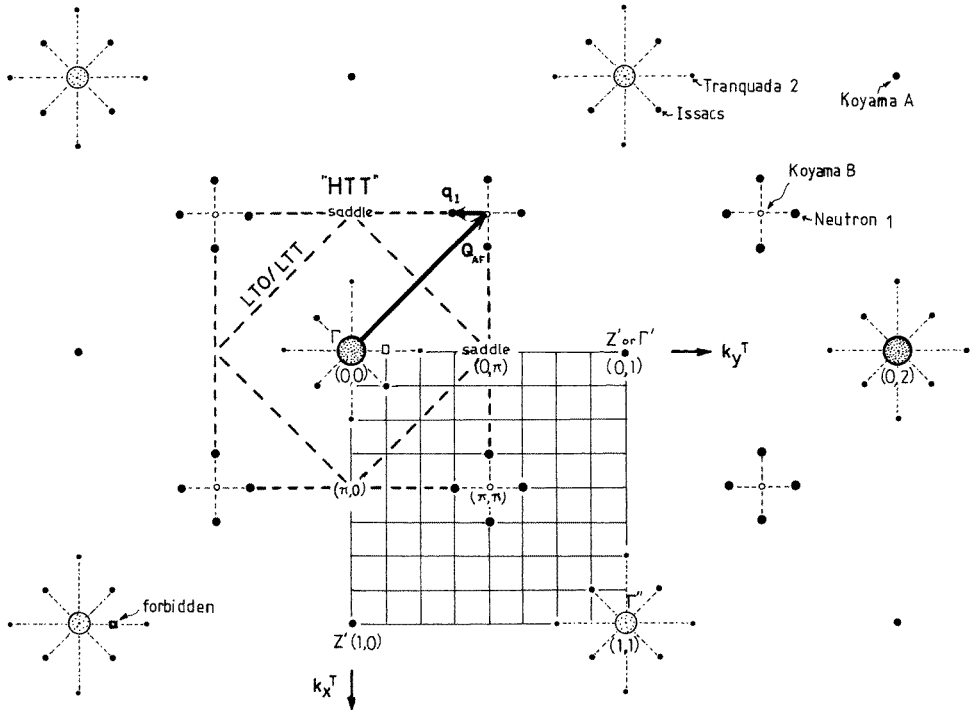

Figure 4. The detailed diffraction pattern (in 2D projection) for $x = 0.125$ LBCO. The strongest spots like (0, 2) are for the basic b.c.t. HTT structure. Spots at Z′, {1, 0}, were termed 'type A' by Koyama *et al* [28] and show up in the LTO and LTT phases; spots at $\{\pi, \pi\}$ are equivalent in 2D and were termed 'type B' by Koyama *et al* [28] who employed electron microscopy. Type B spots have been recorded too by Yamaguchi *et al* using x-rays [29]. The remaining three types of weak spotting come from the domain wall phenomena, and although shown commensurate here to the $8a^T$ geometry become somewhat shifted at other dopings. (i) The four spots around $\{\pi, \pi\}$ are those registered strongly in inelastic neutron spin scattering, and relate primarily to the deviation in the developing spin array from simple antiferromagnetic order. Beware that the deviation wavevector q_I (which yields the wall spacing) often is quoted fractionally in terms of π (i.e. as it relates to Q_{AF}) rather than 2π (and thereby to the basic lattice). These are the spots to which the studies of [11] and [10] in the main refer. (ii) Tranquada *et al* [10] additionally record second-order spots about {2, 0} etc, here marked by very small circles. (iii) The nearby spots marked by somewhat larger closed circles are more interesting in the present context and were first detected by Issacs *et al* [30] working with x-rays. They constitute a combination that monitors the charge aspect of the incipient domain array. If the array were well formed, superlattice spots would arise at a majority of intersections over the fine 1/8 mesh shown. (Useful reference might be made here to the complex diffraction patterns from the discommensurate and higher-order commensurate phases of the layer CDW materials 2H- and 1T-TaS_2 and 2H- and 1T-$TaSe_2$ [31].)

Figure 4 plus its extended caption provide a full summary of the various elements of diffraction information currently available; all are presented here as relates to the 8×8 commensurate condition of figure 1(a). If the real situation were perfectly/statically commensurate, a much fuller array of spotting over the fine 1/8 mesh would be in evidence. Reference might on this point be made to [31] concerning the layered CDW materials 2H- and 1T-TaS_2/$TaSe_2$ in order to appreciate the developments in satellite spotting incurred as a system shifts from incommensurate to discommensurate to fully commensurate organization.

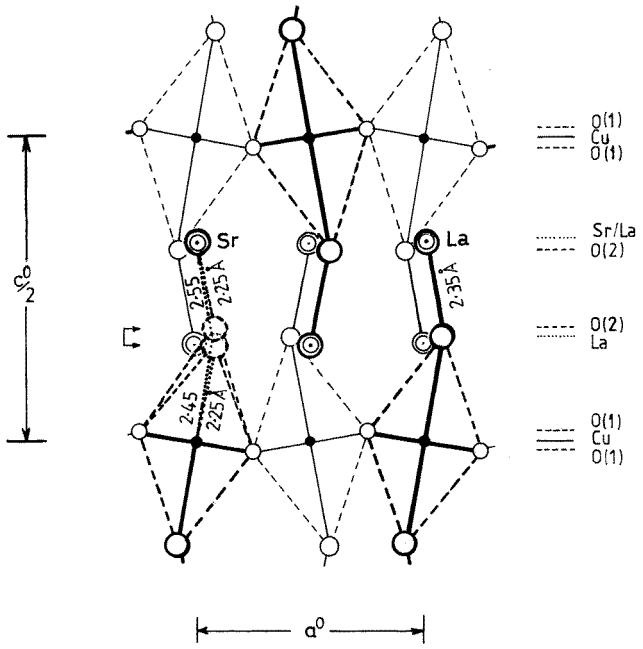

Figure 5. Projection of the LTO LSCO structure down the basal-plane tilt-axis b^O (in *Abma*), emphasizing the 'vertical' Cu–O(2)–Sr/La linkages. EXAFS (see section 3.2) reveals that two clearly different types of position are taken up by O(2) if the end ion is Sr^{2+}, but not where it is La^{3+}. It should be noted here that this particular Sr–O(2) bond in question is the shortest bond within the ninefold-coordination shell of an Sr ion by oxygen. In the LTO phase this shell holds six different site types, having bond lengths ranging from 2.35 up to 2.97 Å in LSCO. In this drawing the tilt of the coordination unit has been doubled for clarity.

Figure 5 presents a view of the LSCO LTO structure looking down the octahedral tilt axis [010]. The apical bond lengths shown are extracted from EXAFS work—see section 3.2.

3. Stripe phase structures

3.1. 1D versus 2D choice

In [1a] when dealing with the HTSC materials the 1D option was never considered since the fourfold-symmetric diffraction data seemed not to warrant it. Furthermore, a 2D modelling allows the charge segregation to be less extreme and the superstructure to be more readily taken up from the random condition. As we have seen in figure 1 the ratio of wall spacing relative to dopant concentration can be rendered identical for the two situations by the use in the 1D case of a doubled charge density. At low dopant concentrations neither situation represents cluster formation. Within the 1D case it could of course be that a crossed geometry arises between successive layers. Certainly a crossed geometry better matches the underlying tetragonal crystal structure, as well as the measured basal isotropy of the electrical and magnetic behaviour, whether within the high- or low-temperature phases.

More recent neutron data have shown now that in fact both types of modelling presented in figure 1 need some modification in the higher-doping regime beyond $x = 1/8$. The natural progression in both previous models would by $x = 1/6$ (i.e. near T_c^{max}) generate

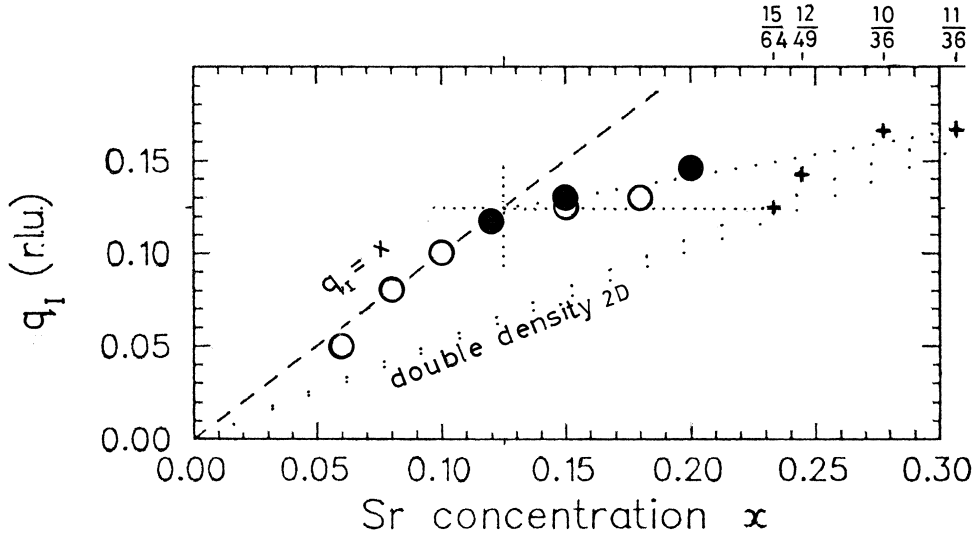

Figure 6. Plotted against hole doping concentration x is the variation of the superlattice wavevector (q_1 of figure 4) as ascertained from neutron scattering—elastic for $(La/Nd/Sr)_2CuO_4$ and inelastic for LSCO itself [33, 32]. The unit gradient found below $x = 1/8$ can be accommodated by 1D stripes at 'doubled density' or by 2D stripes at 'single density'—see figure 1. Beyond $x = 1/8$ the gradient drops by a factor of 4. The extrapolation to (0.306, 0.166) is where a $6a^T$ (square) domain wall would acquire full loading; NB $0.306 = [(2 \times 5) + 1]/6^2$—refer to figure 1 for the counting. Between (1/8, 1/8) and the above point the text introduces the possibility of composites based on $8a^T$ and $6a^T$, as in figure 7, besides intermediate charge loadings. Note that 8×8 at full double density would have a concentration of $[(2 \times 7) + 1]/8^2 = 0.234$, though of course a wavevector of only 0.125.

a domain period of only 24 Å or $6a^T$ (see figure B3 in reference [1a]); recall that the wavevector and concentration in both the above simple models are numerically equal. However, as was noted in [1a] in the discussion of figure B2 concerning the neutron data from $x = 0.140$ LSCO, it looked as though the periodicity might become halted at $8a^T$, with the additional charge then becoming accommodated either centrally to the supercell or at its corner. The new neutron data were obtained by Yamada *et al* who used LSCO [32] and by Tranquada *et al* [33] who worked with Nd-containing LSCO. Their results extend to higher x-values than previously investigated and also identify the superperiod q-values with greater resolution. The employment of Nd substitution in the latter work (whereby static magnetism is, remember, promoted and superconductivity depressed) would appear validated by the agreement found between these two new sets of data. They are plotted together in figure 4(d) of [33] and are reproduced here in figure 6. Indeed they appear to confirm that a $6a^T$ condition never is reached. Rather there occurs a break in the vicinity of $x = 0.125$ away from the numerical identity established at lower x between the wall periodicity wavevector and doping concentration. The new proportionality observed beyond $x = 0.125$ appears diminished by a factor of four. The 2D modelling clearly is able to encompass this crossover by moving towards the double-density charge spacing employed hitherto in the 1D model. However, the latter model possesses no such ready flexibility. Although the new gradient above $x = 0.125$ can readily be incorporated into the 2D modelling, there do emerge still further detailed empirical problems relating to the observed commensuration periods and site-type population ratios.

3.2. Diffraction periodicities, EXAFS and site-type populations

If we proceed to concentrate on the $8a^T$ 2D structure of figure 1(a), there are to a first approximation just two Cu site types there in the ratio 36/64:28/64, divalent:higher-valence; i.e. $56\frac{1}{4}$% are in the former Jahn–Teller-carrying category. It thus was very satisfying when Bianconi *et al* [14b] in 1996 reported from Cu EXAFS work on somewhat underdoped Bi-2212 a clear bimodal distribution of *apical* bond lengths with virtually this ratio (actually $58\frac{1}{2}$%). The BSCCO work was followed by comparable experiments on LSCO ($x = 0.15$). Unfortunately only two data points were included for the latter material above its LTO structural phase transition ($\sim$100 K) [14a]—and this still is so in the more recent elaboration of [14c]. Several observations of significance now need registering here:

(i) the site-type population ratio in LSCO alters upon entry into the LTO phase (T_{d1}), jumping from roughly the above-quoted value at 150 K to almost 75% below T_{d1};

(ii) within the canted LTO structure there now arise, furthermore, two strongly differentiated *basal* Cu–O bond lengths, resulting from the crystal symmetry breakage under coordination-unit tilting;

(iii) the population ratio extracted for these long and short basal Cu–O bonds is significantly different from the associated *apical* ratio;

(iv) for the physically more determinative apical bonds the longer ones shorten somewhat below T_{d1}, while the shorter ones increase;

(v) the various bond lengths, apical and planar, all seem additionally to respond to passage into the LTT condition (T_{d2})—as indeed also through T_c into the superconducting regime. These details need clarifying and the procedure needs repeating for LBCO.

One has to beware at this point of over-interpreting or improperly interpreting the current EXAFS data. For example a strictly bimodal distribution becomes incorporated into the analysis at an early stage. By way of contrast one should note the further subsidiary splitting of the longer apical bond peak recorded from anomalous x-ray diffraction (figure 4 of [34]), which is missing from the EXAFS as presented [14b]. What is more, within the interpretative work by Bianconi *et al* ([14], and references therein) the actual incorporation of the EXAFS data into a structural framework seems to have been based on a false premise. Confusion looks to have arisen concerning the diffraction information employed, and would appear twofold. Firstly, as we have noted, there is the problem that most HTSC structures are based upon a body-centred tetragonal geometry, for which many spots are forbidden (see figure 4). Secondly many of the systems such as the BSCCOs and TBCCOs are very soft along the *c*-axis, and like other layer compounds that are made up of two distinct structural components (e.g. '$BiNbS_3$' [35]) they can display crystallographic misfit behaviour, along with potential long-range lock-in. This mismatch phenomenon leads to the appearance of structural discommensurations (dcs), representing fairly sharp strain-induced phase slippage in an incommensurate mass-density wave. Such behaviour has been imaged directly for BSCCO through areal contrast in dark-field electron microscopy [36]. The images are analogous to those from the Fermi-surface-controlled, incommensurate, charge-density-wave-bearing, group Vb layer dichalcogenides [31, 37]. The latter are orthorhombic in symmetry below their CDW onset temperature, like the majority of HTSC materials. Faulting in these dc arrays leads to very informative compound nodal structures in the images. The misfit arrays are themselves 1D ($1q$) in character for BSCCO, as for '$BiNbS_3$', while the CDWs in TaS_2 etc can present both 1D and 2D ($3q$) dc arrays. The lattice mismatch in BSCCO is quite sizable. Lock-in sometimes has been said to occur at $5b^O$ (NB b^O here is parallel to x', not x; see figure 2). Recent powder neutron work by Miles

et al [38] has revealed that a whole series of micro-adjustments can take place in the basic incommensurate periodicity ($\sim 4.7b^O$ in their sample) upon cooling below 300 K. Now it is the above *rotated* $5b^O$ feature ($\sim$25.5 Å) which Bianconi *et al* mistakenly have employed in construction of their model [14]. As we noted earlier, the correct size of the domain structure is most clearly forthcoming from the neutron spin scattering, and for $x = 0.125$ LSCO is $\sim$31 Å or 16 Cu–O bond lengths, as appears in figure 1(a). Note that the 'Issacs' spots [30] found for LSCO close in around the strong {200} family of charge spots, and incorporated in our figure 4, are indeed 45° rotated with respect to the Cu–O bonds, but this simply indicates a b.c.t. stacking in the supercell (as for the basic structure) between successive Cu layers. Diffraction with the smallest wavevector on the mesh of small squares is then forbidden.

Clearly now it would be invaluable to have comparable EXAFS data for high-quality $Hg_2BaCuO_{4+\delta}$, since this material is not prone to misfit behaviour, and is tetragonal (although b.c.t. again)—not orthorhombic. This request will be reinforced below when we turn to look at other types of data for HBCO.

For the moment let us continue to examine local structural information provided directly from EXAFS data themselves. The beauty of EXAFS is that—as with NMR/NQR—one may specify the atom-site environment under investigation, and moreover, unlike with NMR/NQR, all kinds of central atom are equally eligible for activation. It therefore becomes perfectly possible to examine the above apical shifting of the O(2) oxygen from the other end of its 'vertical' bonding tie-line (figure 5). In LSCO the atoms so placed are the La/Sr. Haskel *et al* [39] recently have reported on just such La and Sr EXAFS, and the information forthcoming provides much insight into the state of structural and electronic organization. The results are as follows.

(i) *Always* the O(2) apical atoms appear at a distance of 2.35 Å from their *La* nearest neighbour.

(ii) By contrast the corresponding *Sr*–O(2) bond length appears highly (and non-thermally) disordered. Further analysis indicates the true situation to be a roughly 50/50 mix of two distinct quasi-equilibrium bond conditions (on an EXAFS versus lattice timescale, $\sim 10^{-15}$ versus 10^{-12} s).

(iii) By incorporating multiple-scattering lengths into the analysis it is found nevertheless that there is a fixed Sr–Cu length which is virtually identical to the La–Cu length. Accordingly the short (2.25 Å) and the long (2.55 Å) Sr–O(2) lengths must directly reflect being near-neighbour in the apical direction to a Cu site well-established in its d^9 J–T condition or in its higher-valence one respectively.

(iv) *Neither* O(2) position here is in the same relation to Sr as the one measured for La; the single (effective) *c*-axis La–O(2) distance in fact falls between the two Sr–O(2) distances, although it is closer to the shorter one.

That the above two Sr–O(2) lengths are significantly different from each other would imply that the observed 50/50 signal sampling ratio should be read as indicating that roughly 50% of the sites O(2) are *frozen* into yielding one type of signal and 50% the other. Where a short Sr–O(2) bond is coupled through 'reciprocally' to a long Cu–O(2) means that this Sr almost permanently has in attendance (to that side) a fully divalent Cu ion. Such a Sr must find itself well inside a domain. The electron deficit automatically incurred must have transferred away to the high-conduction pathways of the regularizing domain boundaries. The other half of the Sr ions, which at $x = 0.15$ find themselves in the vicinity of the boundaries, record a complementary set of Cu ions where the resulting augmented positive charge and high carrier flux have brought about the elimination of the Jahn–Teller distortion.

A glance at the uniform Sr distribution of the 'Wigner' array of figure 3 reveals the above outcome to be one demanding virtually no movement of extra Sr ions onto the domain boundaries. One primarily is witnessing an organization of the holes, not the substituent ions.

Next we have to address why the apical bond-length signal associated with the analogous La sites is so relatively undifferentiated as for only one value to be extracted in the EXAFS analysis, and this placed intermediately between the two associated Sr values. La sites ought on the basis of local charge balance always to be coupled of course to a Cu^{2+} J–T bond, and appropriately therefore the averaged La–O(2) length is indeed well below the mid-point of the two Sr–O(2) values. However, those La atoms happening to find themselves at a domain boundary must clearly not be experiencing the neighbouring presence of the hole carriers for extended periods of time in a way comparable to that for Sr atoms so placed. In other words the conducting pathways are themselves significantly inhomogeneous. It is not surprising accordingly to find that such a conducting framework is one in which evidence of weak localization is apparent in the electrical properties. The $1/T$ behaviour of R_H (and directly the $\rho \sim T$ and the $(\Delta\rho/\rho_o)_H \sim T^{-4}$ behaviour observed for optimally doped materials) has been interpreted upon this basis in reference [1a].

Above, we have been dealing with the La/Sr atoms making record of the charge activity present at the *furthermost* of the two Cu-carrying basal planes by which each such atom is flanked. This I take to be so because the Cu–O changes involved there are longitudinal rather than transverse to the A–O bond under investigation. Furthermore the 'vertical' bond from the La/Sr to the apical O(2) atom is the shortest within the coordination set (figure 5) and hence is the easiest one to isolate from the EXAFS Fourier transform. Clearly in this analysis it always is a tricky matter not to be driven to introduce a superabundant number of free parameters, particularly when remembering that shifts in the position of any one atom will adjust all of its neighbours.

It now would be of considerable interest to see what happens to the *Sr* EXAFS results for LSCO as a function of temperature. What local response might there be to the changes detected at T_{d1} and T_c within the *Cu*-centred EXAFS work of Bianconi *et al* [14a, 14c]?

4. The one-eighth anomaly—clearly a misnomer—but still a mystery?

It is not yet resolved whether there is going to be a somewhat different outcome for charge segregation depending upon just how the source of holes is coordinated into a structure. In HBCO, as in LSCO, the source of holes is sited centrally with respect to four Cu centres in each flanking CuO_2 layer; in $La_2CuO_{4+\delta}$ the excess oxygen sits on a cell edge, while in other compounds such as $Sr_2CuO_2F_{2+\delta}$ [40] it is apical. My impression is that such detail is of distinctly secondary importance to the constructing of HTSC. After all, the superconducting transition temperature ultimately displayed in (bulk segregated) $La_2CuO_{4+\delta}$ [8] is very comparable to that for the cation-substituted LSCO family, and similarly for $YBa_2Cu_3O_6F_2$ [41] it is very much like that for $YBa_2Cu_3O_7$.

The exact level at which one may neglect structural detail of course is a matter of importance when looking for clues wherewith to assess the various contending models for HTSC. Even in bulk crystallographic data that detail continually is growing, coming to express an enormous individuality. Close examination of the recent low-temperature neutron powder diffraction results obtained by Dabrowski *et al* (figure 1 of [20]) for $(La_{2-x}Sr_x)CuO_4$ and $(La_{2-x}Ca_x)CuO_4$ seem to reveal a whole series of slight changes in microstructure as a function of x, of marked variability between the two systems and mostly producing negligible response in T_c. By contrast, the strong dip in T_c present around $x = 0.115$ in

the latter two systems remains *without* comparable expression in the bulk crystallographic behaviour—this markedly different from the case for $(La_{2-x}Ba_x)CuO_4$.

What conceivably could be the origin of these traces of discrete microstructure, especially those beyond $x = 0.125$, given now that, from the new neutron data, q_{av} cannot attain a value of 1/6 prior to an extreme substitution level of $(2\times5)/6^2$ or 0.278, according to the extrapolation made on our figure 6 of the data from figure 4 of Tranquada *et al* [33]. One possibility is that the superstructures themselves become superstructured. Such is a situation not unknown in 'alloy' mass-density waves. Thus in non-stoichiometric $Cu_{3-x}Te_2$ [42] the vacancies segregate out onto planes which then repeat in particular spacing sequences, pppqpppq... etc. Some c-axis stacking not unlike this in high-order staged HTSC systems has locally been resolved by means of HREM [43].

One might between $8a^T$ and $6a^T$ naturally contemplate a simple superstructure based on $7a^T$. From figure 6 this would have to be of composition $(2\times6)/7^2$ or 0.245. However, since we believe that supercells of odd-integer dimension will be energetically disfavoured because the overall pattern of spin-paired square plaquettes is disrupted, use of such a cell is to be disfavoured. An alternative (and one much required in order to attain cell compositions and q-values in the range recorded on figure 6) is accordingly to consider the appearance of composite sequences, made up of $8a^T$ and $6a^T$ units. Thus a $(1\times8)+(1\times6)$ sequence would naturally yield $q_{av} = 1/7$ (or 0.1428), whilst a sequence of $(2\times8)+(1\times6)$ gives 3/22 (or 0.1363). One then would have to 'decorate' the cell edges with charge to a level appropriate to what is indicated in figure 6.

If one were to carry on in this manner to the lower-x side of $8a^T$, the mixed sequence $(2\times8)+(1\times10)$ would yield the situation presented in figure 7. This, for the 'half-density' wall charge shown, takes the composition $(6\times13)/26^2$ and is coupled with an effective q-value of 3/26—both of which equal 0.1154. Accordingly, this we suggest to be the condition for which LSCO (and also LCCO) are at the stage where $T_c(x)$ becomes maximally depressed.

Consistently it is evident from accumulated transport and Meissner measurements (e.g. [23, 25] and references therein) that the anomalies occurring in LSCO in both the normal- and the superconducting-state properties do indeed centre around a somewhat lower x-value than is the case for LBCO. For the latter material the customarily quoted commensurate 1/8 composition/wavevector might suggest that the *lattice* were paramount there. However, when local probe measurements are performed on LBCO etc, such as NMR or μSR, a somewhat different perspective emerges. The anomalies uniformly are revealed as being pre-eminently *electronic* rather than structural in essence. Moreover, prior to superconductivity they appear strongest with regard to q at a value of 0.115—and this surprisingly as much so for LBCO as for LSCO. As noted above both μSR (see [44]) and NMR/NQR (Cu and La; see [23a]) indicate that a new form of local, quasi-static, spin ordering re-emerges at low temperature across the x-range between 1/9 and 1/7. The magnetic order is two dimensional, with the Cu spins themselves lying *in* the basal plane [23a]. The μSR results from Watanabe *et al* [44] show the maximum magnetic ordering temperature in LBCO to be at 35 K, and to occur directly below the maximum in the LTO to LTT symmetry transition of 60 K which arises at $x = 0.125$. The restoration here of tetragonal symmetry, despite showing up as first order and highly hysteretic, is associated with no clear thermodynamic discontinuity and moreover displays no isotope effect [21]. The maxima to *both* above spin and 'charge' events (as distinct from the $T_c(x)$ events) actually would appear even in LBCO to be centred about $x = 0.115$—*not* 0.125 (see figure 3 in [44]). That value of x has been particularly well identified for LSCO by the peak in the linewidth broadening suffered by the $1/2 \leftrightarrow 3/2$ ^{139}La NQR line (see figure 3 in [23a]).

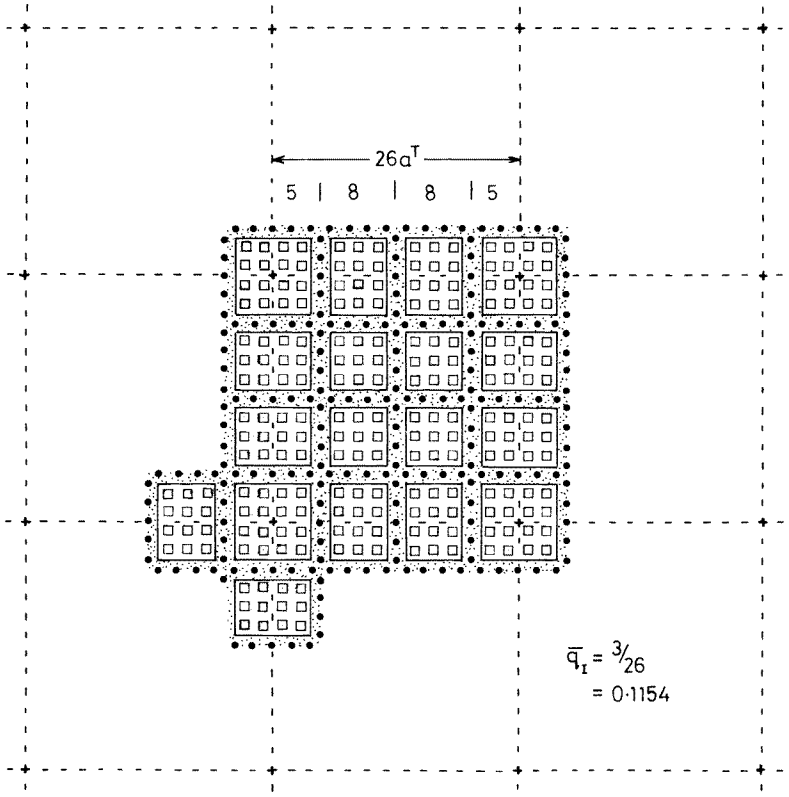

Figure 7. The composite square super-supercell based on $8a^T$ and $10a^T$ designed to yield the point (0.115, 0.115) on figure 6. The four-spin plaquettes are indicated, along with the 'single-density' charge loading of the domain walls. The latter are shown shaded, suppressing the detail of figure 1. Here q_I^{-1} is given by $[(2 \times 8) + (1 \times 10)]/3 = 26/3$, and the charge concentration x for the 26×26 supercell by $(6 \times 13)/26^2$.

Very noteworthy too within the same paper is figure 4, where one witnesses simultaneously a total absence of any influence of the LTO–LTT symmetry transition upon either the NQR linewidths or line frequencies. The site spin and/or the number of sites carrying an ordered moment is not small however—we are not dealing with remnant isolated spins. It soon becomes apparent nonetheless that not all sites can be carrying a 'standard' Cu moment (or indeed an $S = 1/2$ fluctuation-reduced one of 0.6 μ_B as in La_2CuO_4). Looking back in the literature, one may find as early as 1989 that Heffner and Cox, and Weidinger *et al* [45] were in open correspondence concerning the meaning of such odd μSR results for LSCO. From fittings to the line shape and the relaxation data it was argued that these imply the system to be inhomogeneous yet not random. The valence-segregated domain structures now allow insight into how all of the above is possible.

The scenario would proceed as follows. Valence segregation sets in at a considerably higher temperature than the new spin order. That much is witnessed to by the Nd-substituted LSCO elastic neutron diffraction results of Tranquada *et al* [10]. There the presence of Nd stabilizes the appearance of a *static* Cu moment, and yet, even so, sharp magnetic scattering at $(1/2, 1/2-\varepsilon, 0)$ (see the present figure 4) does not show up until a temperature somewhat below that at which organized charge segregation is registered through the $(0, 2-2\varepsilon, 0)$

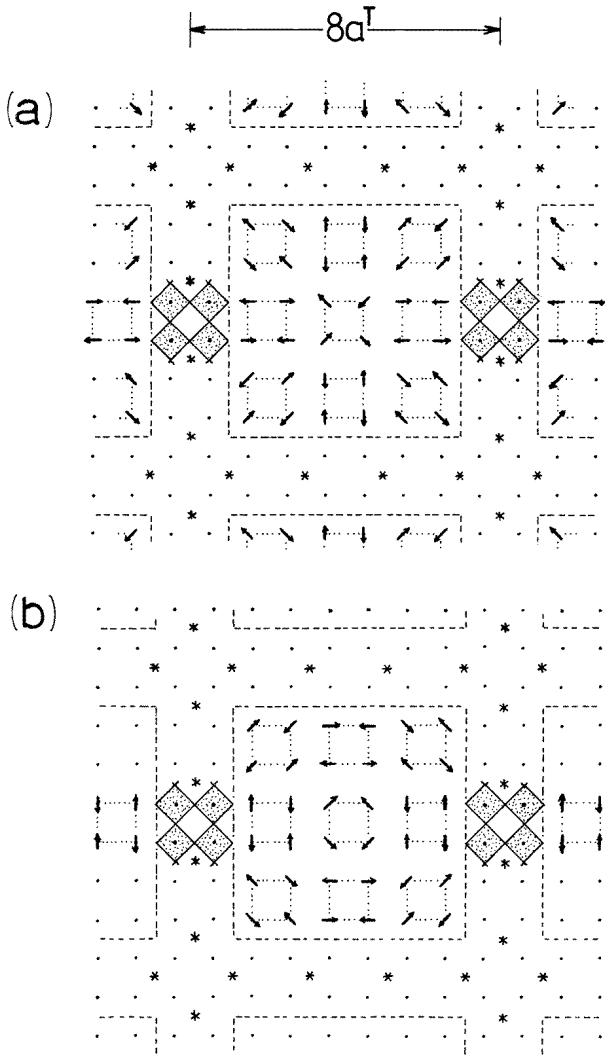

Figure 8. $8a^T$ square domains (at 'single-density' wall loading) showing the possible conformations of the spin orientation as governed by the tilting of the J–T-distorted d^9 octahedra of the inner subsystem relative to the nearby boundary geometry. Wall octahedra are without both spin and J–T apical elongation. The inner spins could also align parallel rather than perpendicular to the domain boundaries, as in the lower section of the figure. In either case the spin arrays are discommensurate across a boundary.

spotting (see figure 4 in [10]). The latter LRO itself develops directly below and most likely inextricably wound up with the LTO/LTT symmetry transition. The LTT condition would seem to emerge in consequence of *some* of the pre-existing coordination-unit tilts being brought into the x- and y-orientations (rather than x' *or* y'), evidently so constrained by consolidation of the 'stripe phase' in the orientations observed. The developing electronic organization effects a restoration thereby in overall tetragonal symmetry to the lattice. This is so despite, at the individual octahedron level, local structural probes such as PDF pointing simultaneously to a high degree of quasi-static 'disorder' within the 'LTT' phase, in the form

of a heavy *mixture* of $0^\circ/90^\circ$ and 45° tilt orientations [46]. This would suggest that the tilt orientation choice for any given (J–T) octahedron is being governed by the latter's immediate conformation to the charged domain boundaries. In turn, the on-site orientation of the (d^9) magnetic moment ordering is very likely being directed magneto-elastically to follow the octahedral tilt orientation taken up locally. Accordingly one may anticipate that within an 8×8 domain the inner d^9 spin-plaquette array will present a Union Jack type of form as portrayed by figure 8. A comparable though somewhat less splayed array would occur for the 10×10 domains. Such spin arrays hold to the requirement of being discommensurate in spin orientation across the domain boundaries. The above would account for why the superlattice structure manages so strongly to be evident in neutron spin scattering, whether inelastic as with LSCO [10] or elastic as when Nd doped [11]. Note in concluding that octahedral tilting at the unit-cell level is observed to be not entirely eliminated even above T_{d1} within the HTT phase [47]—and nor, of course, from the neutron work, is the tendency toward valence segregation.

One very sensitive way to examine the global aspects of a complex circumstance like the above is the use of ultrasound ($\sim$10 MHz). Indeed Sakita, Nohara and co-workers [48], using very high quality LSCO crystals of well specified x, have obtained remarkable results as a function of temperature and composition, and additionally incorporating the action of a magnetic field up to 14 T. Their results are reproduced now as figure 9 accompanied by the original description. The experiment which reveals a strongly x-specific anomalous softening in the transverse shear elastic modulus ($\frac{1}{2}(C_{11} - C_{12})$; B_{2g} in b.c.t. D_{4h}^{17}) is set up with a transverse wave propagating in the [110] direction. The shear strain involved stretches and compresses the Cu–O basal bonds but without change in the area of the CuO_2 units. The magnetic field is applied in the c-direction. From this work the following points should be noted carefully:

(i) the softening, centred on $x = 0.115$, develops at a composition where the modulus actually is greatest;

(ii) the maximum softening in the modulus is less than $\frac{1}{2}$%;

(iii) the softening starts from the LTO–LTT transition (60 K), and hardens up again at the lowest temperatures;

(iv) at $x = 0.113$ the softening is totally unperturbed by the application of the magnetic field, whereas the superconductivity becomes greatly suppressed;

(v) the situation by the time $x = 0.138$ is reached is substantially different, since the softening now requires the assistance of the magnetic field to bring it about; also T_c is much less suppressed.

Pursuing the domain picture, I would attribute the enhanced rigidity at $x = 0.113$ to the presence of the charge-carrying walls, with the observed softening once below T_{d2} as due to carrier freeze-out there. The general loss of metallicity is reversed only by the residual superconductivity. By the time $x = 0.138$ is reached the rapid drift away from the ionic limit and local magnetism is such that now the external field is required to restrict charge motion. With $x = 0.19$ the system becomes too metallic for the domain structure to be well defined. At the other end of the scale at $x = 0.09$ the carrier concentration is too dilute to dominate the response of the system, and indeed the application of the magnetic field now somewhat hardens it. Clearly it would be good at this point to have data for further intermediate compositions, and also comparable data for LBCO when suitable crystals become available.

The effect above of an applied magnetic field in enhancing the anomaly is similar to what is secured in LSCO and LBCO by the addition of Nd [27, 33]. It is to be viewed as the counter-effect to applied pressure. Pressure helps generally to delocalize the system,

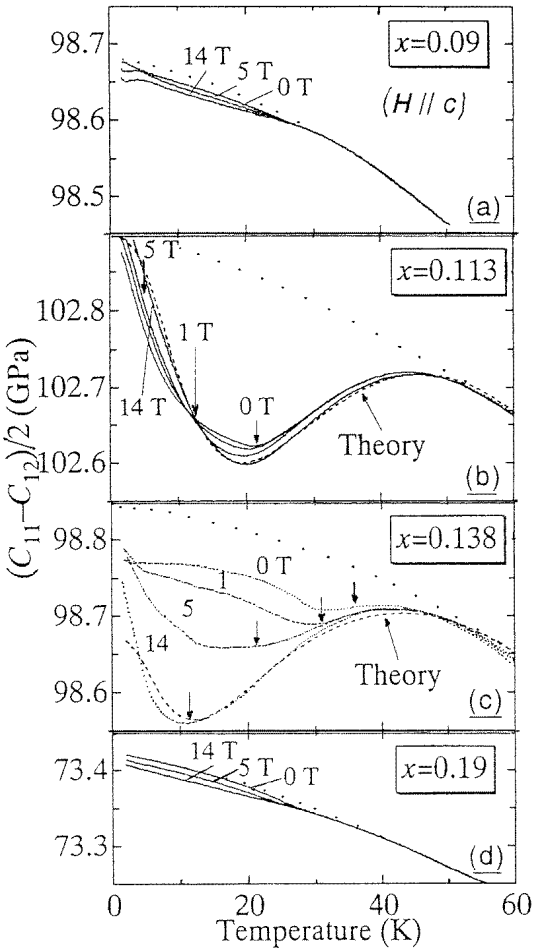

Figure 9. The transverse elastic modulus $(C_{11} - C_{12})/2$ of $(La_{2-x}Sr_x)CuO_4$ at (a) $x = 0.090$, (b) $x = 0.113$, (c) $x = 0.138$ and (d) $x = 0.190$. The vertical arrows in (b) and (c) indicate $T_c(H)$. No superconducting transition is observed for $x = 0.113$ at 14 T. Each dashed curve in (b) and (c) is a fit with 2D vHS very slightly offset from E_F (by the equivalent of 37 and 25 K respectively). From Sakita *et al* [48]. (I have sketched in the pre-softened extrapolations of the moduli.)

narrow the anomaly, and even decrease somewhat the x-value about which it is centred. The application of pressure is known rapidly to eliminate the LTT condition (by 0.5 GPa), this permitting T_c to rise somewhat [49], and the anomaly actually is reported to contract in upon $x = 0.125$ [50]. Several other Japanese groups have examined the situation for LBCO in great detail and they observe that under ordinary conditions the maximum suppression of T_c occurs not at 1/8 but at somewhat greater values of x up to 0.136 [51, 52]. Indeed Takayama-Muromachi *et al* have registered a double dip in T_c centred upon the x-values of 0.115 and 0.136 [51], values which above we have tentatively identified as relating to simple 2-to-1 composites of 1/8 with 1/10 and with 1/6 respectively. Doubtless this added disorder assists with carrier localization (as also might some incipient CDW-type nesting from side to side of *individual* saddle points on the Fermi surface).

5. Density-of-states peaks, correlation, negative-U states and HTSC

It is illuminating to see how Sakita *et al* [48] attempt to account for the ultrasound anomaly at $x = 0.113$. A fitting is undertaken by turning to the logarithmic singularity of a strictly 2D DOS; it is treated as closely pinned to E_F and subsequently becomes shear strain split. To obtain a final hardening at the lowest temperatures it is found necessary in fact to introduce a very slight offset of the pre-split peak from E_F by $\sim$2.5 meV ($\equiv$30 K). This is the same sort of contrived circumstance as was postulated in several recent attempts to interpret the anomalous Seebeck coefficient results for HTSC materials. The approach has been criticized at length in [1c] as being inappropriate to the circumstances. The band-structural complexities of the various HTSC systems are too distinct from each other for the communality of their observed physical behaviour to have to relate *at this level* to detail within standard one-electron density-of-states profiles. As Obertelli *et al* [53] some time ago demonstrated, almost all of the Seebeck data can be reduced onto a virtually universal plot for the various HTSC systems. This matter very recently has been addressed theoretically by Hildebrand and co-workers [54] taking a much more general approach based on a highly correlated tight-binding formulism. In this the Hubbard U-parameter is dealt with using the FLEX (fluctuation-exchange) technique, wherein temperature and both spin and charge fluctuations are incorporated. The results prove remarkably capable of matching the absolute magnitudes as well as temperature dependencies of the observed Seebeck coefficients. Moreover the detailed treatment is able also to identify why in the LSCO family alone the coefficient fails to become negative at high temperatures: this derives from the unique reverse curvature of the Fermi surface in k-space for this family. The above success in modelling the thermoelectric data is not governed by very sharp DOS peaks in the band structure by chance 'correctly' placed with respect to E_F: in reality there is no such detail comparable to that occurring in 'bare' tight-binding single-band modelling. The relevant many-body density-of-states profile in fact displays a pseudogap in proximity to E_F which arises in consequence of the spin- and charge-gap correlation phenomena—now at last being more widely addressed in regard to HTSC matters.

Why I would not endorse the above work in its entirety, and think it still little more than a first step in the right direction, lies with the grossly oversimplified model band structure being taken as adequate for the cuprates and more particularly the HTSC phenomenon; note in consequence the restricted interpretation which then can be placed upon U. It will be observed from my earlier papers [1] on cuprate HTSC that I believe that the latter will support a primarily electronic negative-U interpretation of events. However, such an outcome requires the inclusion of the entire p/d-band complex, and in particular the effects from d-shell closure—not to mention the two-subsystem behaviour. Double-occupancy fluctuations then readily arise. It is the positioning of these correlated fluctuational states in close proximity to E_F which is seen as being responsible in large measure for the characteristic normal-state transport behaviour (as well as ultimately HTSC) within the existing inhomogeneous environment of the layered mixed-valence cuprates [1c].

Very relevant then in the above paper from Hildebrand *et al* is that to reach their promising fittings to the Seebeck data they have to insert a numerically very small value of $U = 1$ eV (taking $U = 4t$ with $t = 0.25$ eV and thereby making $U \sim W$). Such a value of U is much smaller than that called for by a material like NiO ($\sim$5 eV or more). Within the framework employed by Hildebrand *et al*, U cannot be carried through below zero. There, $U = 0$ is the equivalent of a correlation-free system, rather than being where two strong correlation terms cancel. The value of U which has been foreseen in [1] is ~ -1 eV per electron, this placing the negative-U state very close to E_F at precisely the stage at which

T_c becomes maximized in HTSC systems—namely $x = 1/6$ (figure 1 in [1c]).

The above sort of correlation-driven electronic origin to HTSC is at a considerable distance then from those interpretations which would rely simply upon an extreme density-of-states peak at E_F for advancing either a standard phononic coupling interpretation of HTSC or a spin-fluctuation-based one. Such treatments entirely avoid the basic question 'Why cuprates alone?'

In a recent treatment by Gyorffy and co-workers [55] a tight-binding LMTO approach, based upon the Andersen *et al* eight-band parametrization of the crucial CuO_2 planes using a quality LDA band structure for $YBCO_7$, has been carried forward into the Kohn–Sham–Bogoliubov–de Gennes superconductivity equations themselves. The hope pursued is that the pairing kernel might itself, in the present small-ξ circumstances of HTSC, support a corresponding parametrization in real-space orbital terms, and thereby help to locate the seat of the carrier pairing interaction. The latter is taken as being non-retarded. One by one, the various candidate orbital pairings were tried out to supply the observed T_c, and it was found, within the framework employed, that this most readily is accomplished under nearest-neighbour $d_{x^2-y^2}$–$d_{x^2-y^2}$ pairing interaction. The latter was somewhat preferred over the corresponding *on-site* d–d interaction. Such an outcome might be taken to support say an RVB-driven pairing process in preference to the negative-U shell-closure process advocated above. Considered individually, the former process is demonstrated to lead to a d-wave gap symmetry, while the latter would be s wave. However, as has been observed previously, these calculations have been carried through still under the premise that the system is homogeneous. In the real mixed-valence/stripe phase environment one has to recognize that the pairing interaction is not homogeneously distributed, but highly local, and a single-order-parameter description is then inappropriate. As discussed in section 9 of [1a], this inhomogeneity in order parameter and coherence length lies at the root of the conundrum that the c-axis tunnelling is able to appear as s-wave-like [56] and thereby quite different from the planar tunnelling with its strongly d-wave-like expression. Clearly it now is essential to attempt to broaden the basis of the above already difficult calculations and to incorporate at least a CPA-type two-site alloy treatment. It has also to be remarked that, as currently constituted, the considerable initial success of the above paper is too open to being perceived as the product of a standard van Hove singularity; remember that by every measure the metal and its Fermi surface are far from standard. A much more highly correlated treatment appears called for, as demonstrated by Hildebrand *et al* [54].

Where the density-of-states argument in support of HTSC has been carried to an extreme is in the papers of Bianconi and co-workers, under the heading of 'shape resonance' [57]. Embracing the existence of a striped microstructure, they have suggested that what drives forward the HTSC phenomenon is the piling up of an extreme, quantal transverse superstructure, DOS peak on the top of a standard free-electron DOS peak, now of 1D ε^{-1}-form. They have proceeded by use of the Kramers–Krönig model, and insert a sharp superlattice potential well of depth nearly 1/2 eV in order to boost T_c up to the required level. This is done while at the same time maintaining standard weak coupling ($\lambda = 0.25$) with a quite low energy cut-off of 50 meV (as if HTSC were lattice (or spin) governed). The above would seem a particularly unrealistic way to proceed, since, as we have seen, where superstructures are most strongly formed around $x = 1/8$, there T_c becomes most depressed, and where T_c is highest, it is there that the isotope effect becomes strongly suppressed.

My own belief is that what the (incipient) stripe phase formation succeeds in introducing is a local structure wherein the divalent and trivalent subsystems become more highly defined, yet at the same time remaining highly interspersed and open to cross-communication of both single carriers and pairs. Moreover the structuring of the divalent subsystem into

spin-gapped RVB plaquettes is especially beneficial in limiting spin-wave pair breaking at the high temperatures involved. What is more, as emphasized in [1a], the pre-existing RVB electron pairs are readily able to be taken over onto the negative-U sites of the domain boundaries, there to be stabilized further into a superconductive pairing with coherence running over the entire system. In return, the back-flowing *hole* pairs might very well propagate through the RVB-coupled array of each domain interior.

If, in these ways, striped charge segregation is able (away from where longitudinally it can become Fermi surface commensurate) to be of real benefit to the advancement of T_c, it would be proper to seek further direct evidence of its presence in HTSC systems other than those for which T_c these days is not too exciting. In the accompanying paper [58], we do just that, showing again the Seebeck coefficient to be a particularly useful means of tracking T_c as oxygen is withdrawn from superoxygenated samples. As with LSCO, the dip that we have discovered in $T_c(\delta)$ for the system $HgBa_2CuO_{4+\delta}$ looks to be centred somewhat below the hole count $p = 1/8$. Comparable behaviour has lain hidden among many other existing data, including the EXAFS results for BSCCO-2212 from Bianconi *et al* [14b] discussed above. Indeed it is demonstrably the true origin of the famous 'double-plateau' behaviour seen in $YBa_2Cu_3O_y$. There one ought not so much to perceive a plateau at $y = 6\frac{2}{3}$ as a dip at $6\frac{3}{4}$. To a first approximation we are tracking the 'linearized' pair of sequences

$y = 6.45 \quad 6.55 \quad 6.65 \quad 6.75 \quad 6.85 \quad 6.95$ (total oxygen stoichiometry)

versus

$p = 0.040 \quad 0.065 \quad 0.090 \quad \underline{0.115} \quad 0.140 \quad 0.165$ (planar hole content).

This has nicely been confirmed by Tallon *et al* [59] through making the double adjustment to the Cu valence afforded by the system $(Y/Ca)Ba_2Cu_3O_{6+z}$. The T_c-dip tracks the net hole content, not the oxygen stoichiometry. The latter would be the case were the oxygen chain ordering at $6\frac{2}{3}$ playing the dominant role in controlling T_c across this range. Of course the chains (and the associated strong orthorhombicity) do there complicate other matters significantly [60]. Now surely tetragonal single-layer $HgBa_2CuO_{4+\delta}$ has to constitute the better material around which to frame future experimental and calculational work.

In summary then, the subject of mixed-valence charge segregation has been further examined. The self-organized microstructural details have been explored including 1D/2D crossover. Neutron and EXAFS results have provided the basis for this analysis. The Jahn–Teller effect must be recognized as a crucial element in the 'charge/spin'-separation structuring. On cooling, the emergent RVB-type magnetic organization of the divalent subsystem assists greatly in preparing if not pre-pairing the overall system for high-temperature superconductivity. Under the action of the negative-U centres of the high-valence subsystem, established in the domain boundaries, the overall system can evolve naturally with doping and cooling from $d_{x^2-y^2}$ towards greater s-wave-type content of the HTSC order parameter.

Note added in proof. I would like to draw to the attention of the readers two substantial reviews recently published bearing directly on the above material in journals not regularly carrying HTSC papers: Markiewicz [62] and Ovchinnikov [63].

References

[1a] Wilson J A and Zahrir A 1997 *Rep. Prog. Phys.* **60** 941
[1b] Wilson J A 1997 *Nature* submitted

[1c] Wilson J A 1997 *J. Phys.: Condens. Matter* **9** 6061 (erratum **9** 8793)
[1d] Wilson J A 1994 *Physica* C **233** 332
[1e] Wilson J A 1989 *Int. J. Mod. Phys.* B **3** 691
[1f] Wilson J A 1988 *J. Phys. C: Solid State Phys.* **21** 2067
Wilson J A 1987 *J. Phys. C: Solid State Phys.* **20** L911
[1g] Wilson J A 1988 *Proc. NATO Advanced Research Workshop on Narrow Band Phenomena (NATO ASI Series B, vol 184)* ed J C Fuggle, G A Sawatsky and J W Allen (New York: Plenum) pp 209–13
[2a] Yoshimura K, Imai T, Shimizu T, Ueda Y, Kosuge K and Yasuoka H 1989 *J. Phys. Soc. Japan* **58** 3057
[2b] Song Y-Q, Kennard M A, Lee M, Poeppelmeier K R and Halperin W P 1991 *Phys. Rev.* B **44** 7159
[2c] See also
Fujiyama S, Itoh Y, Yasuoka H and Ueda Y 1998 *J. Phys. Soc. Japan* at press
[3] Mustre de Leon J, Conradson S D, Batistic I and Bishop A R 1990 *Phys. Rev. Lett.* **65** 1675
[4] Egami T, Dmowski W, McQueeney R J, Sendyka T R, Ishihara S, Tachiki M, Yamauchi H, Tanaka S, Hinatsu T and Uchida S 1996 *Phil. Mag.*
[5] Edwards P P, Peacock G B, Hodges J P, Asab A and Gameson I 1997 *HTSC 10 Years after Discovery (NATO ASI Series B)* ed E Kaldis and E Liarokapis (Dordrecht: Kluwer) pp 135–76
[6a] Pickett W E 1989 *Rev. Mod. Phys.* **61** 433
[6b] Novikov D L, Mryasov O N and Freeman A J 1994 *Physica* C **222** 38
[7a] Wilson J A 1972 *Adv. Phys.* **21** 143
[7b] Wilson J A 1984 *The Electronic Structure of Complex Systems (NATO ASI Series B, vol 113)* ed P Phariseau and W M Temmerman, pp 657–708
[7c] Wilson J A 1985 *Metallic and Non-metallic States of Matter* ed P P Edwards and C N Rao (London: Taylor and Francis) ch 9
[8] Ryder J, Midgley P A, Exley R, Beynon R J, Yates D L, Afalfiz L and Wilson J A 1991 *Physica* C **173** 9
[9] Chou F and Johnston D C 1996 *Phys. Rev.* B **54** 572
[10] Tranquada J M, Sternlieb B J, Axe J D, Nakamura Y and Uchida S 1995 *Nature* **375** 561
[11] Mason T E, Aeppli G, Hayden S M, Ramirez A P and Mook H A 1993 *Phys. Rev. Lett.* **71** 919 and references therein
[12a] Littlewood P B 1990 *Phys. Rev.* B **42** 10 075
[12b] Littlewood P B, Zaanen J, Aeppli G and Monien H 1993 *Phys. Rev.* B **48** 487
[13a] Varma C M and Weber W 1986 *Phys. Rev.* B **19** 4809
[13b] Withers R L and Wilson J A 1986 *J. Phys. C: Solid State Phys.* **19** 4809
[14a] Bianconi A, Saini N L, Lanzara A, Missori M, Rosetti T, Oyanagi H, Yamaguchi H, Oka K and Ito T 1996 *Phys. Rev. Lett.* **76** 3412
[14b] Bianconi A, Saini N L, Rosetti T, Lanzara A, Perali A, Missori M, Oyanagi H, Yamaguchi H, Nishihara Y and Ha D H 1996 *Phys. Rev.* B **54** 12 018
[14c] Saini N L, Lanzara A, Oyanagi H, Yamaguchi H, Oka K, Ito T and Bianconi A 1997 *Phys. Rev.* B **55** 12 759
[15a] Pickett W E, Cohen R E and Krakauer H 1992 *Proc. Conf. on Lattice Effects in High T_c Superconductors (Santa Fe, NM, 1992)* ed Y Bar-Yam, T Egami, J Mustre de Leon and A J Bishop (Singapore: World Scientific) p 217
[15b] Cohen R E, Pickett W E, Papaconstantopoulos D and Krakauer H 1992 *Proc. Conf. on Lattice Effects in High T_c Superconductors (Santa Fe, NM, 1992)* ed Y Bar-Yam, T Egami, J Mustre de Leon and A J Bishop (Singapore: World Scientific) pp 223–8
[15c] Krakauer H, Pickett W E and Cohen R E 1992 *Proc. Conf. on Lattice Effects in High T_c Superconductors (Santa Fe, NM, 1992)* ed Y Bar-Yam, T Egami, J Mustre de Leon and A J Bishop (Singapore: World Scientific) pp 229–34
[15d] Mazin I I, Andersen O K, Liechtenstein A I, Jepsen O, Antropov V P, Rashkeev S N, Anisimov V I, Zaanen J, Rodriguez C O and Methfessel M 1992 *Proc. Conf. on Lattice Effects in High T_c Superconductors (Santa Fe, NM, 1992)* ed Y Bar-Yam, T Egami, J Mustre de Leon and A J Bishop (Singapore: World Scientific) pp 235–51
[16a] Axe J D 1992 *Proc. Conf. on Lattice Effects in High T_c Superconductors (Santa Fe, NM, 1992)* ed Y Bar-Yam, T Egami, J Mustre de Leon and A J Bishop (Singapore: World Scientific) pp 517–30
[16b] Axe J D and Crawford M K 1994 *J. Low Temp. Phys.* **95** 271
[16c] Wu T and Fossheim K 1993 *Phys. Rev.* B **48** 16 751
[17a] Maki M, Sera M, Hiroi M and Kobayashi N 1996 *Phys. Rev.* B **53** 11 324
[17b] Kitazawa K, Nagano T, Nakayama Y and Kishio K 1993 *Appl. Supercond.* **1** 567
[18] Billinge S J L, Kwei G H, Lawson A C, Thompson J D and Takagi H 1993 *Phys. Rev. Lett.* **71** 1903

[19] Norman M R, Mullen G J, Novikov D L and Freeman A J 1993 *Phys. Rev.* B **48** 9935
[20] Dabrowski B, Wang Z, Rogacki K, Jorgensen J D, Hitterman R L, Wegner J L, Hunter B A, Radaelli P G and Hinks D G 1996 *Phys. Rev. Lett.* **76** 1348
This paper backtracks on this matter, but presents some very interesting structural data to be discussed later relating to layer flatness.
[21] Frank J P and Lawrie D D 1995 *J. Supercond.* **8** 591
[22] Radaelli P G, Hinks D G, Mitchell A W, Hunter B A, Wagner J L, Dabrowski B, Vanderwoort K G, Viswanathan H K and Jorgensen J D 1994 *Phys. Rev.* B **49** 4163
[23a] Ohsugi S 1995 *J. Phys. Soc. Japan* **64** 3656
[23b] Maki M, Sera M, Hiroi M and Kobayashi N 1996 *Phys. Rev.* B **53** 11 324
See reference [21] for a comparable situation in $(La/Ca)_2CuO_4$.
[24] Maeno Y, Kakehi N, Tanaka Y, Tomita T, Nakamura F and Fujita T 1992 *Proc. Conf. on Lattice Effects in High T_c Superconductors (Santa Fe, NM, 1992)* ed Y Bar-Yam, T Egami, J Mustre de Leon and A J Bishop (Singapore: World Scientific) pp 542–7
[25] Moodenbaugh A R, Wildgruber U, Wang Y L and Xu Y 1995 *Physica* C **245** 347
[26] Crawford M K, Farneth W E, Harlow R L, McCarron E M, Miao R, Chou H and Huang Q 1992 *Proc. Conf. on Lattice Effects in High T_c Superconductors (Santa Fe, NM, 1992)* ed Y Bar-Yam, T Egami, J Mustre de Leon and A J Bishop (Singapore: World Scientific) pp 531–41
Kawano K, Kumagai K, Watanabe I, Nishiyama K and Nagamine K 1994 *Physica* B **194–6** 351
[27] Wagener W, Klauss H-H, Hillberg M, de Melo M A C, Birke M, Litterst F J, Buchner B and Micklitz H 1997 *Phys. Rev.* B **55** R14 761
[28] Koyama Y, Wakabayashi Y, Ito K and Inoue Y 1995 *Phys. Rev.* B **51** 9045
[29] Yamaguchi H, Ito T, Oka K and Oyanagi H 1995 *J. Phys. Soc. Japan* **64** 3614
[30] Issacs E D, Aeppli G, Zschack P, Cheong S-W, Williams H and Buttrey D J 1994 *Phys. Rev. Lett.* **72** 3412
[31] Wilson J A, DiSalvo F J and Mahajan S 1975 *Adv. Phys.* **24** 117
Withers R L and Wilson J A 1986 *J. Phys. C: Solid State Phys.* **20** 4809
Wilson J A 1985 *J. Phys. C: Solid State Phys.* **15** 591
Wilson J A 1990 *J. Phys.: Condens. Matter* **2** 1683
[32] Yamada K 1998 to be published
(Results quoted in [33].) Now partially released in
1998 *Phys. Rev.* B **57** R3229
[33] Tranquada J M, Axe J D, Ichimura N, Moodenbaugh A R, Nakamura Y and Uchida S 1997 *Phys. Rev. Lett.* **78** 338
[34] Bianconi A, Lusignoli M, Saini N L, Bordet P, Kvick A and Radaelli P G 1996 *Phys. Rev.* B **54** 4310
[35] Gotoh Y, Akimoto J, Goto M, Oosawa Y and Onoda M 1995 *J. Solid State Chem.* **116** 61
Otero-Diaz L C, Withers R L, Gomez-Herrero A, Welberry T R and Schmid S 1995 *J. Solid State Chem.* **115** 274
[36] Clin M, El Boussiri K, Henocque J, Schneck J, Toledano J C, Portemer F and Morin D 1997 *Physica* C **280** 9
[37] McKernan S, Steeds J W and Wilson J A 1982 *Phys. Scr.* T **1** 74
Fung K K, McKernan S, Steeds J W and Wilson J A 1981 *J. Phys. C: Solid State Phys.* **14** 5417
[38] Miles P A, Kennedy S J, Anderson A R, Gu G D, Russell G L and Koshizuka N 1997 *Phys. Rev.* B **55** 14 632
The high complexity of Bi(III) oxide stereochemistry is also presented in
Miles P A, Kennedy S J, Anderson A R, Gu G D, Russell G L and Koshizuka N 1997 *Phys. Rev.* B **56** 5662
[39] Haskel D, E. Stern A, Hinks D G, Mitchell A W and Jorgensen J D 1997 *Phys. Rev.* B **56** R521
Haskel D, Stern E A, Hinks D G, Mitchell A W, Jorgensen J D and Budnick J L 1996 *Phys. Rev. Lett.* **76** 439
[40] Bhargava S C and Wani B N 1996 *Solid State Commun.* **99** 825
[41] Shpanchenko R V, Rozova M G, Abakumov A M, Ardashnikova E I, Kovba M L, Putilin S N, Antipova E V, Lebedev O I and Van Tendeloo G 1997 *Physica* C **280** 272
[42] Colaitis D, van Dyck D, Delavignette P and Amelinckx S 1980 *Phys. Status Solidi* a **58** 271
[43] Akimoto J, Tokiwa K, Iyo A, Ihara H, Hayakawa H, Gotoh Y and Oosawa Y 1997 *Physica* C **273** 181
[44] Watanabe I, Kawano K, Kumagai K, Nishiyama K and Nagamine K 1992 *J. Phys. Soc. Japan* **61** 3058
[45] Heffner R H and Cox D L 1989 *Phys. Rev. Lett.* **63** 2538
Weidinger A, Niedermayer C, Golnik A, Simon R and Recknagel E 1989 *Phys. Rev. Lett.* **63** 2539
[46] Billinge S J L and Kwei G H 1996 *J. Phys. Chem. Solids* **57** 1457

[47] Dmowski W, McQueeney R J, Egami T, Feng Y P, Sinha S K, Hinatsu T and Uchida S 1995 *Phys. Rev.* B **52** 6829
and also note
Zhu Y, Moodenbaugh A R, Cai Z X, Tafto J, Suenaga M and Welch D O 1995 *Phys. Rev.* B **52** 6829
relating to micro-twinning.
[48] Sakita S, Suzuki T, Nakamura F, Nohara M, Maeno Y and Fujita T 1996 *Physica* B **219+220** 216
[49] Katano S, Funahashi S, Mori N, Ueda Y and Fernandez-Baca J A 1993 *Phys. Rev.* B **48** 6569
[50] Yamada N and Ido M 1992 *Physica* C **203** 240
[51] Takayama-Muromachi E, Izumi F and Kamayama T 1993 *Physica* C **215** 329
[52] Yamada Y, Sera M, Sato M, Takayama T, Takata T and Sakata M 1994 *J. Phys. Soc. Japan* **63** 2314
[53] Obertelli S D, Cooper J P and Tallon J L 1992 *Phys. Rev.* B **46** 14 928
[54] Hildebrand G, Hagenaars T J, Hanke W, Grabowski S and Schmalian J 1997 *Phys. Rev.* B **56** R4317
[55] Gyorffy B L, Szotek Z, Temmerman W M, Andersen O K and Jepsen O 1998 *Phys. Rev.* B at press
[56a] Sun A G, Truscott A, Katz A S, Dynes R C, Veal B W and Gu C 1996 *Phys. Rev.* B **54** 6734
[56b] Kleiner R, Katz A S, Sun A G, Summer R, Gajewski D A, Han S, Woods S I, Dantsker E, Chen B, Char K, Maple M B, Dynes R C and Clarke J 1996 *Phys. Rev. Lett.* **76** 2161
[57] Bianconi A, Valetta A, Perali A and Saini N L 1997 *Solid State Commun.* **102** 369
[58] Farbod M and Wilson J A 1998 in preparation
See
Farbod M 1998 *PhD Thesis* University of Bristol
[59] Tallon J L, Bernhard C and Shaked H 1995 *Phys. Rev.* B **51** 12 911
NB This paper and related ones confuse the onset of SRO AFM behaviour with the magnetic pseudogap. The former relates to the stiffening of the magnetic subsystem registered through a decrease in spin susceptibility, whereas the latter is associated with RVB plaquette coupling and the shedding of small-q, low-energy spin excitations as the magnetic subsystem becomes highly fragmented by the developing domain structure (see figure 2 in [1a]).
[60] Tallon J L, Bernhard C, Binninger U, Hofer A, Williams G V M, Ansaldo E J, Budnick K I and Niedermeyer C 1995 *Phys. Rev. Lett.* **74** 1008
[61] Burrow J H, Maule C H, Strange P, Tothill J N and Wilson J A 1987 *J. Phys. C: Solid State Phys.* **20** 4115
[62] Markiewicz R S 1997 *J. Phys. Chem. Solids* **58** 1179
[63] Ovchinnikov S G 1997 *Sov. Phys.–Usp.* **40** 993